Cancer Therapy: Preclinical

Clinical Cancer Research

Dual CDK4/CDK6 Inhibition Induces Cell-Cycle Arrest and Senescence in Neuroblastoma

JulieAnn Rader[1], Mike R. Russell[1], Lori S. Hart[1], Michael S. Nakazawa[1], Lili T. Belcastro[1], Daniel Martinez[2], Yimei Li[1,3], Erica L. Carpenter[1], Edward F. Attiyeh[1,3], Sharon J. Diskin[1,3], Sunkyu Kim[5], Sudha Parasuraman[5], Giordano Caponigro[5], Robert W. Schnepp[1], Andrew C. Wood[1], Bruce Pawel[2], Kristina A. Cole[1,3], and John M. Maris[1,3,4]

Abstract

Purpose: Neuroblastoma is a pediatric cancer that continues to exact significant morbidity and mortality. Recently, a number of cell-cycle proteins, particularly those within the Cyclin D/CDK4/CDK6/RB network, have been shown to exert oncogenic roles in neuroblastoma, suggesting that their therapeutic exploitation might improve patient outcomes.

Experimental Procedures: We evaluated the effect of dual CDK4/CDK6 inhibition on neuroblastoma viability using LEE011 (Novartis Oncology), a highly specific CDK4/6 inhibitor.

Results: Treatment with LEE011 significantly reduced proliferation in 12 of 17 human neuroblastoma-derived cell lines by inducing cytostasis at nanomolar concentrations (mean $IC_{50} = 307 \pm 68$ nmol/L in sensitive lines). LEE011 caused cell-cycle arrest and cellular senescence that was attributed to dose-dependent decreases in phosphorylated RB and FOXM1, respectively. In addition, responsiveness of neuroblastoma xenografts to LEE011 translated to the *in vivo* setting in that there was a direct correlation of *in vitro* IC_{50} values with degree of subcutaneous xenograft growth delay. Although our data indicate that neuroblastomas sensitive to LEE011 were more likely to contain genomic amplification of *MYCN* ($P = 0.01$), the identification of additional clinically accessible biomarkers is of high importance.

Conclusions: Taken together, our data show that LEE011 is active in a large subset of neuroblastoma cell line and xenograft models, and supports the clinical development of this CDK4/6 inhibitor as a therapy for patients with this disease. *Clin Cancer Res; 19(22); 6173–82. ©2013 AACR.*

Introduction

Neuroblastoma is a pediatric cancer that originates in tissues of the developing sympathetic nervous system. It is typically diagnosed in very young children and has a highly variable clinical presentation, with tumors displaying significant genomic and biological heterogeneity (1–3). Although patients with favorable clinical and biological features (low-risk disease) can often be cured by surgery alone, patients with high-risk disease, particularly those harboring amplification of the *MYCN* oncogene, have survival rates of less than 40% despite intensive multimodal therapy (1, 4). Such high mortality thus mandates a need for the development of novel therapies that will significantly improve high-risk patient survival.

The identification of molecular abnormalities driving neuroblastoma tumorigenesis and disease progression followed by their targeted treatment is a pragmatic strategy for meeting this need. Currently, converging evidence points to members of the Cyclin D/CDK4/CDK6/RB cell-cycle regulatory pathway as potential candidates for such therapeutic exploitation. Both *CDK4* and *CDK6* (*CDK4/6*) encode cyclin-dependent serine–threonine kinases that, in response to mitogenic or pro-proliferative stimuli, complex with D-type cyclins to phosphorylate the RB tumor suppressor protein. This phosphorylation induces the release of RB from E2F transcription factors, and thus enables E2F to transcribe the genes that are required for G_1–S phase cell-cycle progression and ultimately cellular proliferation (5–7). In addition to cell-cycle regulation, CDK4/6 signaling has also been linked to senescence suppression via regulation of the FOXM1 transcription factor (8). Given its demonstrated ability to override suppressive cues in favor of cellular proliferation, it is not surprising that deregulation of the Cyclin D/CDK4/CDK6/RB pathway is associated with unrestricted growth and is a hallmark of nearly every tumor histotype.

Authors' Affiliations: [1]Division of Oncology and Center for Childhood Cancer Research; [2]Division of Pathology, Children's Hospital of Philadelphia; [3]Department of Pediatrics; [4]Abramson Family Cancer Research Institute, Perelman School of Medicine at the University of Pennsylvania, Philadelphia, Pennsylvania; and [5]Novartis Institutes for Biomedical Research, Cambridge, Massachusetts

Note: Supplementary data for this article are available at Clinical Cancer Research Online (http://clincancerres.aacrjournals.org/).

Corresponding Author: John M. Maris, Children's Hospital of Philadelphia, Colket Translational Research Building, Room 3060, 3501 Civic Center Blvd., Philadelphia, PA 19104. Phone: 215-590-5244; Fax: 267-426-0685; E-mail: maris@email.chop.edu

doi: 10.1158/1078-0432.CCR-13-1675

Translational Relevance

Neuroblastoma is a pediatric cancer that continues to exact significant morbidity and mortality. We and others have shown that the Cyclin D/CDK4/CDK6/RB pathway is hyperactive in neuroblastoma, suggesting that this cancer might be particularly vulnerable to CDK4/6 inhibition. In an effort to translate this finding to the clinic, we evaluated the *in vitro* and *in vivo* response of neuroblastoma to LEE011 (Novartis Oncology), a small molecule inhibitor targeting CDK4 and CDK6. We show that a majority of neuroblastoma models are indeed sensitive to CDK4/6 inhibition, with sensitivity attributed to an induction of cytostasis (G_1 arrest) and cellular senescence. Our data therefore strongly support the integration of CDK4/6 inhibitors into current treatment regimens for neuroblastoma, and have provided a rationale for initiating a phase I clinical trial in this disease (NCT01747876).

With respect to neuroblastoma, we and others have identified several genetic aberrations that increase CDK4/6 kinase activity. Genomic amplification of *CCND1* (Cyclin D1) and *CDK4*, as well as homozygous deletion of *CDKN2A*, have been reported in a subset of neuroblastomas (9–14). In addition, *CCND1*, *CDK4*, and *CDK6* have not only been shown to be overexpressed in almost all cases of neuroblastoma, but also their expression was found to be higher in neuroblastoma in comparison to other tumors (15). More recently, a synthetic lethality screen of the protein kinome identified CDK4 as a potential candidate for therapeutic targeting in neuroblastoma (16). Taken together, these findings suggest a dependency on CDK4/6 activity for neuroblastoma survival, and thus highlight their potential as molecular targets for pharmacologic inhibition.

LEE011 (Novartis Oncology) is an orally bioavailable, small molecule inhibitor of both CDK4 and CDK6. Here, we report on the preclinical evaluation of LEE011 as a neuroblastoma therapy. Our results show that a subset of neuroblastomas are highly sensitive to LEE011, and therefore support the clinical development of CDK4/6 inhibition strategies in this disease.

Materials and Methods

Cell lines and patient samples

All cell lines were obtained from the Children's Hospital of Philadelphia cell line bank and were cultured in RPMI-1640 media containing 10% FBS, 1% L-glutamine, and 1% penicillin/streptomycin at 37°C and 5% CO_2. Annual genotyping (AmpFISTR Identifier Kit) of these lines and a single-nucleotide polymorphism (SNP) array analysis (Illumina H550) were performed to ensure maintenance of cell identity using methods as previously described (17). All annotated but de-identified patient tumor samples were obtained from the Children's Oncology Group neuroblastoma biorepository. The Illumina H550 SNP arrays were used to determine DNA copy number status of 375 high-risk primary neuroblastoma tumors, and gene expression profiling of 251 tumors (30 low-risk, 221 high-risk) was performed using Affymetrix Human Exon 1.0 ST microarrays.

Tissue microarray

A neuroblastoma tissue microarray of duplicate paraffin-embedded tumor cores from 106 diagnostic patients, as well as control tissues, was used for this study (18). Using the Bond Refine polymer staining kit (Leica Microsystems), slides from each tumor core were stained with an antibody against endogenous RB (Cell Signaling #9309, 1:300 dilution). Antigen retrieval was performed with E2 retrieval solution (Leica Microsystems), and developed slides were imaged at 20× magnification on an Aperio OS slide scanner (Aperio Technologies). Positive staining was described by staining intensity (negative, weak, moderate, or strong), and a staining score was also calculated as the product of staining intensity and the percentage of neuroblasts stained.

Western blotting

Approximately 40 μg of cell line or patient tumor lysate was prepared as previously described (19), separated by electrophoresis on 4% to 12% polyacrylamide gels (Lonza), transferred to PVDF membranes (Millipore), and probed with primary antibodies at the indicated dilutions: RB, 1:2,000; pRB^{S780}, 1:2,000; pRB^{S795}, 1:2,000; $pRB^{S807/811}$, 1:2,000; Cyclin D1, 1:1,000; Cyclin D3, 1:1,000; MYCN, 1:1,000; FOXM1, 1:1,000 (Cell Signaling); CDK4, 1:2,000; CDK6, 1:3,000; and β-Actin, 1:3,000 (Santa Cruz). All blots were quantified with ImageJ (National Institutes of Health).

RNA interference

Cell lines were plated in triplicate in 96-well plates, and knockdown of *CDK4* and *CDK6* was performed 24 hours later via combined transfection with 25 nmol/L ON-TARGET SMARTpool siRNA targeting *CDK4* and 25 nmol/L ON-TARGET SMARTpool siRNA targeting *CDK6* (Thermo Scientific). Cell lines were also transfected with siRNAs directed against PLK1 as well as nontargeting oligonucleotides (NTC), representing positive and negative controls, respectively. Cell viability was assayed 72 hours posttransfection using *Cell Titer Glo* (Promega). Gene knockdown was confirmed to be >85% at this time point by quantitative real-time PCR, and protein-level knockdown was confirmed by Western blot.

Pharmacologic growth inhibition

LEE011 was provided by Novartis pharmaceuticals. A panel of neuroblastoma cell lines, selected based upon prior demonstration of substrate adherent growth, was plated in triplicate on the Xcelligence Real-Time Cell Electronic Sensing system (ACEA Biosciences) and treated 24 hours later with a four-log dose range of inhibitor or with a

dimethyl sulfoxide (DMSO) control. Cell indexes were monitored continuously for ~100 hours, and IC_{50} values were determined as follows: growth curves were generated by plotting the cell index as a function of time and were normalized to the cell index at the time of treatment for a baseline cell index of 1. The area under the normalized growth curve from the time of treatment to 96 hours posttreatment was then calculated using a baseline area of 1 (the cell index at the time of treatment). Areas were normalized to the DMSO control, and the resulting data were analyzed using a nonlinear log inhibitor versus normalized response function (GraphPad Prism). All experiments were repeated at least once.

Cell-cycle analysis

Cell lines were plated in duplicate in 35 mm plates and treated 24 hours later with the indicated concentrations of LEE011 or with a DMSO control. At 96 hours posttreatment, cells were gently harvested and fixed overnight in 70% ethanol. Cells were then washed in PBS, stained with 1 μg/μL FxViolet Stain (Invitrogen), and assayed for DNA content on an Attune Acoustic Focusing Cytometer (Invitrogen). Analysis was carried out using VenturiOne software (Applied Cytometry).

Senescence and apoptosis assays

Cellular senescence was assayed via measurement of senescence-associated β-galactosidase activity (SA-β-gal). Cells were grown for 24 hours in 35 mm plates, treated with 500 nmol/L LEE011 for 6 days, and then fixed and stained overnight according to the manufacturer's protocol (Cell Signaling #9860). Cells were then imaged for SA-β-gal using an Axio Observer D.1 phase contrast microscope (Zeiss). The percentage of SA-β-gal positive cells was determined by counting the number of positive cells present in 3 separate microscope frames, and then normalizing to the control. To assess apoptotic activity, cells were plated in triplicate in 96-well plates, treated with LEE011, and assayed for caspase 3/7 activation 16 hours after treatment with Caspase-Glo 3/7 (Promega). Cells treated with SN-38 were used as a positive control (20).

Xenograft therapeutic trials

The BE2C, NB-1643, or EBC1 cell line–derived xenografts were implanted subcutaneously into the right flank of CB17 $SCID^{-/-}$ mice. Animals bearing engrafted tumors of 200 to 600 mm^3 were then randomized to oral treatment with 200 mg/kg LEE011 in 0.5% methylcellulose ($n = 10$) or vehicle ($n = 10$) daily for a total of 21 days. Tumor burden was determined periodically throughout treatment according to the formula $(\pi/6) \times d^2$, where d represents the mean tumor diameter obtained by caliper measurement. In accordance with the Children's Hospital of Philadelphia Institutional Animal Care and Use Committee, animals were euthanized as soon as tumor volume exceeded 3 cm^3. A linear mixed effects model was used to analyze differences in the rate of tumor growth between the LEE011 and vehicle-treated groups.

Immunohistochemistry of xenografted neuroblastomas

$pRB^{S807/811}$ (Cell Signaling) or Ki67 (Abcam #16667) antibodies were used to stain slides of formalin-fixed, paraffin-embedded tumor that had been excised from mice following 7 days of treatment with vehicle or LEE011. Staining for $pRB^{S807/811}$ was performed in accordance with the manufacturer's protocol (Cell Signaling) using a 1:200 dilution of primary antibody followed by a 1:500 dilution of anti-rabbit immunoglobulin G (IgG) secondary antibody (Abcam # 6721). Slides pretreated with alkaline-phosphatase (New England Biolabs) were used to confirm specificity of phosphorylation detection. For Ki67 staining, slides were incubated in a pressure cooker (Biocare Medical) with antigen unmasking solution (Vector Labs H3300), blocked with 2% FBS and endogenous biotin (Vector Labs SP2001), and stained at a 1:400 dilution of primary antibody for 1 hour and a 1:200 dilution of biotinylated anti-rabbit IgG secondary antibody (Vector Labs) for 30 minutes. Slides were then developed via incubation with ABC (Vector Labs) for 30 minutes followed by DAB (DAKO Cytomation) for 10 minutes. All slides were counterstained with Harris Hematoxylin (Fisher Scientific), dehydrated, mounted, and imaged at 20× magnification with an Aperio OS slide scanner (Aperio Technologies).

Results

CDK4/6 signaling is hyperactive in neuroblastoma

Copy number gain and overexpression of *CDK4*, *CDK6*, and *CCND1* have been reported in many neuroblastoma cell lines (refs. 10–15; Supplementary Table S1). To confirm that these genomic aberrations translate to constitutive CDK4/6 signaling within the Cyclin D/CDK4/CDK6/RB pathway, we examined the activation status of RB in a comprehensive panel of highly characterized human neuroblastoma-derived cell lines. As shown in Fig. 1A, robust phosphorylation of RB at serines 780 and 807/811—residues directly targeted by CDK4 and CDK6 (21–23)—was observed in all neuroblastoma cell lines, and protein-level expression of CDK4, CDK6, and Cyclin D1 occurred in the majority of lines. Comparatively, RB phosphorylation together with protein-level expression of CDK4, CDK6, and Cyclin D1 was substantially lower in several other representative tumor types as well as in immortalized, nontransformed retinal pigmented epithelial (RPE1) cells (Fig. 1B). Thus, it seems that in neuroblastoma cell lines, aberrant overexpression of *CDK4*, *CDK6*, and *CCND1* does indeed facilitate hyperactive CDK4/6 signaling within the Cyclin D/CDK4/CDK6/RB network.

We next analyzed several neuroblastoma patient samples to verify that the pathway activation observed in neuroblastoma cell lines is also a characteristic of patient tumors at diagnosis and is not simply an artifact of the *in vitro* setting. We found that *CDK4* mRNA was highly expressed in high-risk patients in comparison to low-risk patients, and we observed copy number gain of *CDK4* (5.1%), *CDK6* (15.7%), and *CCND1* (19.5%) in a cohort of 375 high-risk

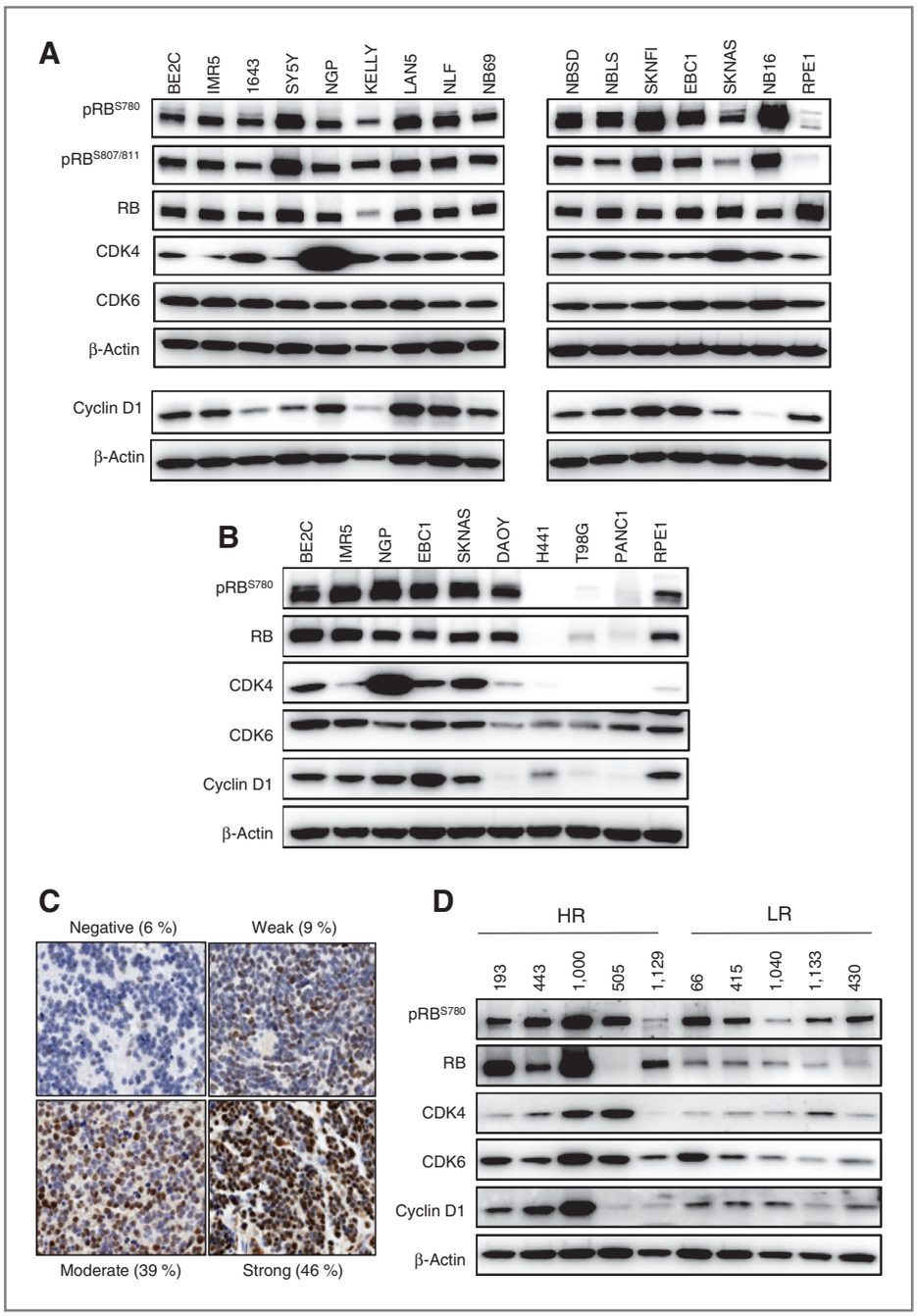

Figure 1. The Cyclin D/CDK4/CDK6/RB pathway is hyperactive in neuroblastoma. A, Western blot analysis of a panel of neuroblastoma cell lines reveals high protein expression of CDK4, CDK6, and Cyclin D1 as well as extensive phosphorylation of RB that (B) is higher in neuroblastoma lines in comparison to nontransformed RPE1 cells and several pediatric and adult tumor types. DAOY, medulloblastoma; H441, lung adenocarcinoma; T98G, glioblastoma multiforme; PANC1, pancreatic carcinoma. Diagnostic tumors from neuroblastoma patients also demonstrate constitutive pathway activation, as evidenced by (C) intense positive staining of a neuroblastoma tissue microarray for RB and (D) Western blot analysis of high-risk and low-risk tumors.

patients (Supplementary Fig. S1 and Table S2). RB was also expressed in the majority of patients, as a tissue microarray comprised of 106 diagnostic tumors revealed that 100 (94%) stained positively for total endogenous RB, with 90 (85%) showing moderate to strong staining (Fig. 1C). A significant increase in RB staining intensity, however, was observed in high-risk, *MYCN* amplified samples ($P = 0.03$; Supplementary Fig. S2). Western blot analysis of several diagnostic tumor samples confirmed the expression of CDK4, CDK6, and CCND1 protein, and also indicated the presence of active, phosphorylated RB (Fig. 1D). These data therefore demonstrate that CDK4/6 signaling is indeed hyperactive in both neuroblastoma cell lines and tumors.

A large subset of neuroblastoma cell lines is sensitive to CDK4/6 inhibition

Due to our observation that CDK4/6 signaling is highly active in neuroblastoma (15, 16), thus maintaining hyperphosphorylated RB and supporting cell-cycle progression through the G_1–S checkpoint, we chose to interrogate the

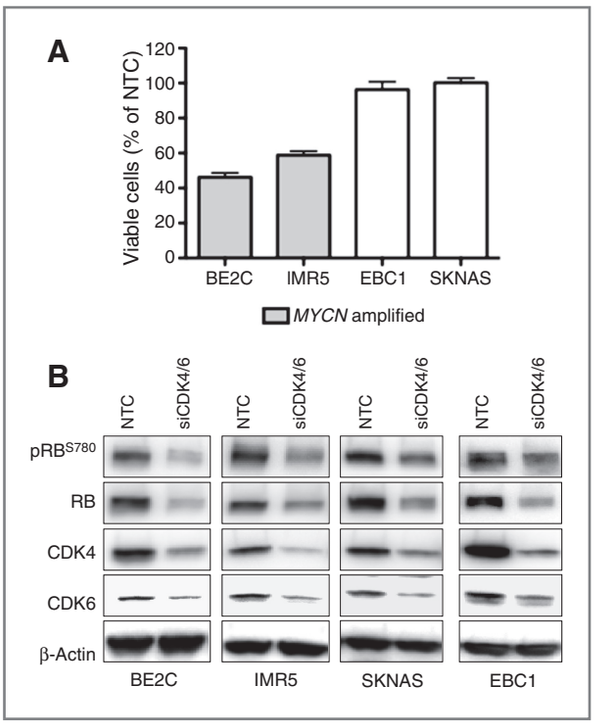

Figure 2. Dual siRNA-mediated knockdown of *CDK4* and *CDK6* inhibits neuroblastoma growth. A, siRNA-mediated knockdown of both CDK4 and *CDK6* expression significantly reduced neuroblastoma growth in a manner that correlated with *MYCN* status ($P = 0.03$). Cell viabilities are expressed as the percentage of NTC. B, representative protein depletion of CDK4, CDK6, and pRB^{S780}.

effect of dual CDK4/6 depletion on neuroblastoma cell lines. Targeted depletion of CDK4/6 by siRNA resulted in differential decreases in cell viability, where some lines responded robustly to CDK4/6 depletion whereas little to no effect was observed in other lines (Fig. 2A). This phenotypic stratification of cell lines into CDK4/6 "sensitive" or "resistant" was not due to knockdown efficiency, as we achieved significant knockdown of *CDK4* and *CDK6* mRNA and protein in all cell lines (Fig. 2B). Sensitive cell lines, however, were more likely to harbor amplification of *MYCN* ($P = 0.03$; Fig. 2A).

We next investigated whether pharmacologic inhibition of CDK4/6 phenocopied siRNA-mediated protein depletion by treating a panel of 17 neuroblastoma cell lines with LEE011 across a four-log dose range (10–10,000 nmol/L). Treatment with LEE011 significantly inhibited substrate adherent growth relative to the control in 12 of the 17 neuroblastoma cell lines examined (mean $IC_{50} = 306 \pm 68$ nmol/L, considering sensitive lines only, where sensitivity was defined as an IC_{50} of less than 1 μmol/L; Fig. 3A). This differential sensitivity to pharmacologic CDK4/6 inhibition largely reflected that of CDK4/6 depletion by siRNA, in that *MYCN* amplified cell lines were more sensitive to LEE011 than nonamplified lines ($P = 0.01$; Fig. 3A) and cell line *MYCN* expression was inversely correlated with sensitivity ($r = -0.55$, $P = 0.03$; Supplementary Fig. S3). To confirm that the growth inhibition observed in sensitive cell lines was indeed because of a targeted impairment of CDK4/6 signaling, we analyzed the levels of phosphorylated RB following treatment with LEE011. Depletion of pRB^{S780} was observed as early as 6 hours posttreatment in the BE2C and IMR5 cell lines, both of which respond to LEE011 with growth inhibition at nanomolar IC_{50} values (data not shown). This effect was sustained at 96 hours, with depletion of pRB^{S780} beginning at 250 nmol/L. Decreased pRB^{S780} was also seen in the EBC1- and SKNAS-resistant cell lines, however only at higher inhibitor concentrations (Fig. 3B).

CDK4/6 inhibition induces cytostasis that is mediated by G_1 arrest and senescence

Analysis of the real-time substrate adherent growth curves generated by LEE011 treatment of neuroblastoma cell lines showed that growth inhibition in sensitive cell lines was consistent with a cytostatic effect (data not shown). However, because responses to targeted inhibition of cyclin-dependent kinase pathways are not always strictly a result of cell-cycle arrest (24–26), we sought to fully characterize the mechanism of neuroblastoma growth inhibition in response to pharmacologic CDK4/6 inhibition. LEE011 treatment of 2 neuroblastoma cell lines (BE2C and IMR5) with demonstrated sensitivity to CDK4/6 inhibition resulted in a dose-dependent accumulation of cells in the G_0/G_1 phase of the cell cycle (Fig. 4A). This G_0/G_1 arrest became significant at inhibitor concentrations of 100 nmol/L ($P = 0.007$) and 250 nmol/L ($P = 0.01$), respectively, and was also accompanied by dose-dependent decreases in the percentage of cells in S and G_2–M. As expected, cell lines that were resistant to CDK4/6 inhibition arrested in G_1 only at significantly higher doses of LEE011 (EBC1, 5 μmol/L, $P = 0.01$; SKNAS, no arrest achieved; Fig. 4A and B).

Recently, a systematic screen for novel CDK4/6 substrates identified the FOXM1 transcription factor as a potential target of CDK4/6 signaling, and implicated CDK4/6-mediated activation of FOXM1 in the prevention of cellular senescence (8, 25, 27–29). These results are corroborated by the fact that FOXM1 inhibition, either by deletion or by CDK4/6 inhibition, impairs the self-renewal capacity of cells (29). We therefore investigated whether or not inhibition of CDK4/6 activity by LEE011 would induce senescence in neuroblastoma via downregulation of FOXM1. There was a significant reduction in *FOXM1* mRNA as early as 6 hours following administration of LEE011 to sensitive cell lines, and modest but reproducible decrease in FOXM1 protein levels (Fig. 4C and D). This was associated with the induction of cellular senescence in sensitive lines, as indicated by a significant increase in the percentage of SA-β-gal positive cells (Fig. 4E). By contrast, cell lines resistant to LEE011 showed no reduction of *FOXM1* mRNA or protein following LEE011 treatment, and subsequently did not senesce. As we did not observe significant increases in caspase 3/7 activity or PARP cleavage in sensitive lines treated with LEE011 (Supplementary Fig. S5), these results

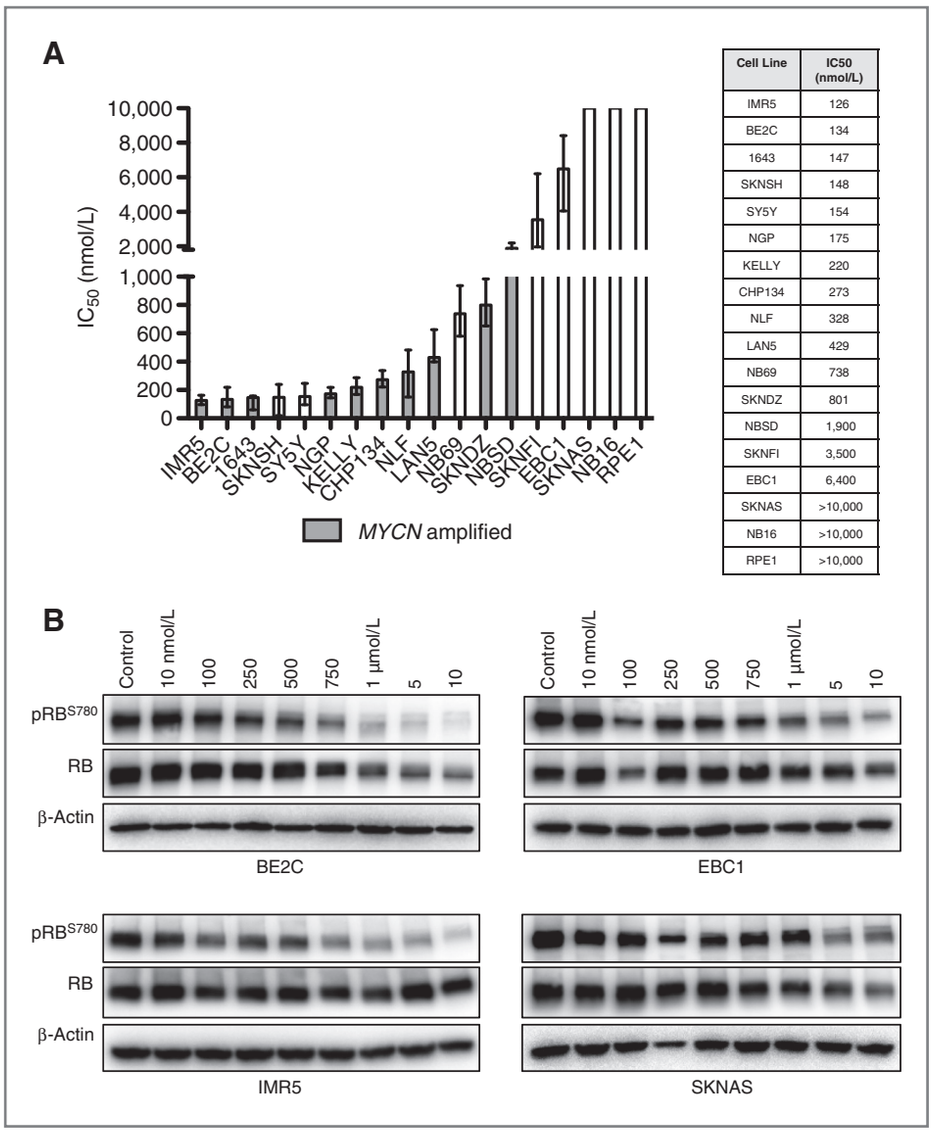

Cell Line	IC50 (nmol/L)
IMR5	126
BE2C	134
1643	147
SKNSH	148
SY5Y	154
NGP	175
KELLY	220
CHP134	273
NLF	328
LAN5	429
NB69	738
SKNDZ	801
NBSD	1,900
SKNFI	3,500
EBC1	6,400
SKNAS	>10,000
NB16	>10,000
RPE1	>10,000

Figure 3. Pharmacologic inhibition of CDK4/6 suppresses neuroblastoma growth *in vitro*. A, the growth of 12 of 17 neuroblastoma cell lines was significantly impaired in response to CDK4/6 inhibition with LEE011 (mean $IC_{50} = 306 \pm 68$ nmol/L, sensitive lines only). Data are plotted (and tabulated) as the best fit IC_{50} per log(inhibitor) versus normalized response analysis (GraphPad Prism); upper and lower bars represent 95% confidence levels. B, dose-dependent decreases in pRB^{S780} accompany growth suppression in sensitive lines and are indicative of on-target activity.

suggest that the growth inhibition of neuroblastoma cell lines following CDK4/6 inhibition is primarily cytostatic and is mediated by a G_1 cell-cycle arrest and cellular senescence.

CDK4/6 inhibition causes tumor growth delay *in vivo*

Given the observed differential sensitivity of neuroblastoma cell lines to CDK4/6 inhibition, we assayed for *in vivo* efficacy using neuroblastoma cell line–derived xenografts representing the extremes of *in vitro* sensitivity. CB17 immunodeficient mice bearing BE2C, NB-1643 (*MYCN* amplified, sensitive *in vitro*), or EBC1 (nonamplified, resistant *in vitro*) xenografts were treated once daily for 21 days with LEE011 or with a vehicle control. This dosing strategy was well tolerated, as no weight loss or other signs of toxicity were observed in any of the xenograft models. As shown in Fig. 5A and Supplementary Fig. S6, tumor growth was significantly delayed throughout the 21 days of treatment in mice harboring the BE2C or 1643 xenografts (both, $P < 0.0001$), although growth resumed posttreatment (data not shown). By contrast, as anticipated by the *in vitro* data, tumor growth suppression was less robust in the EBC1 xenograft model ($P = 0.51$). Assessment of the Ki67 proliferation marker by immunohistochemistry confirmed that proliferation was impaired only in the BE2C and 1643 xenograft models, as tumors resected from separate cohorts of BE2C or 1643 xenografted mice demonstrated comparatively weaker staining following 7 days of treatment with LEE011 than with the vehicle control, whereas no Ki67 staining differences were observed in the EBC1 xenografts (Fig. 5B). Phosphorylation of RB was also substantially diminished in the BE2C and 1643 xenografts, whereas only a minimal decrease was detected in the EBC1 model (Fig. 5B and C).

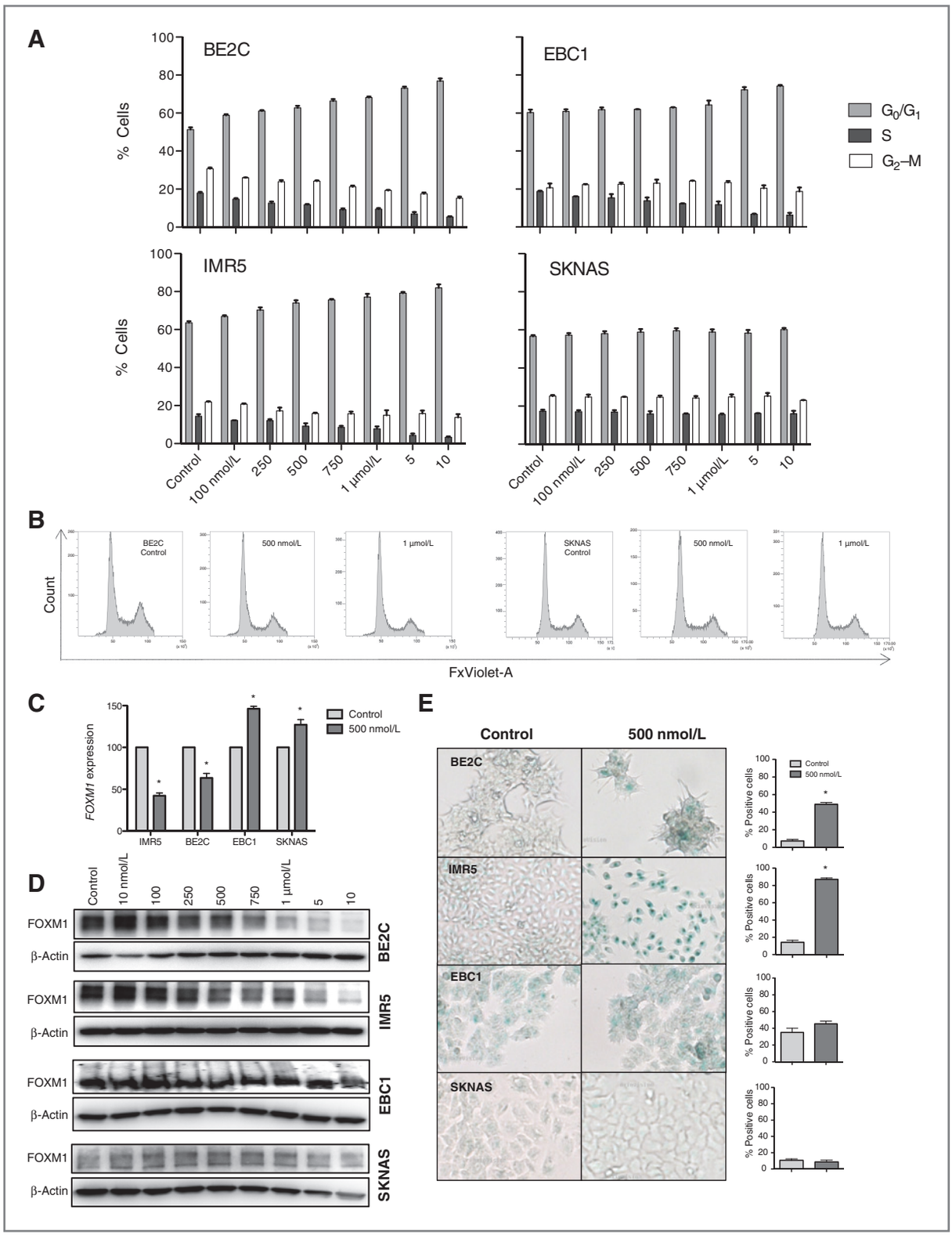

Figure 4. Growth suppression via CDK4/6 inhibition is mediated by cell-cycle arrest and senescence. Neuroblastoma cell lines with demonstrated sensitivity or resistance to LEE011 were analyzed for cell-cycle arrest and SA-β-gal activity. A, a significant G_1 arrest accompanied by reductions in the fraction of cells in S-phase and G_2–M was observed in sensitive lines only. B, representative cell-cycle histograms of a sensitive and resistant cell line. C, downregulation of *FOXM1* mRNA $^*P = 0.02$ and (D) protein was observed in sensitive lines and was associated with (E) the induction of a senescent phenotype ($^*P = 0.0001$).

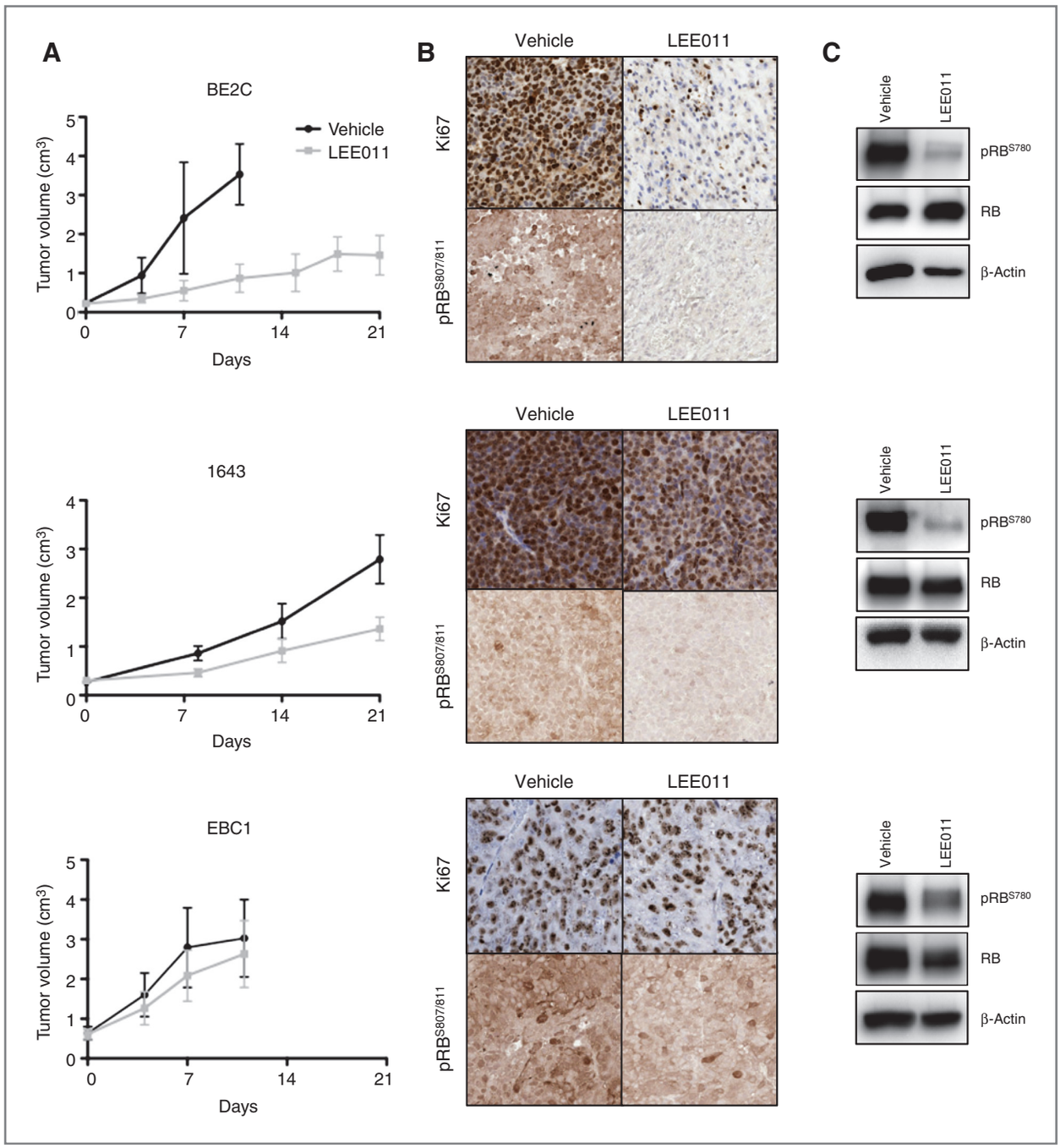

Figure 5. Inhibition of CDK4/6 suppresses neuroblastoma growth *in vivo*. A, mice with subcutaneously implanted xenografts were treated daily with 200 mg/kg LEE011 or with a vehicle for 21 days. In 2 of 3 neuroblastoma xenograft models, treatment with LEE011 significantly reduced tumor burden in comparison to vehicle, as determined by linear mixed effects analysis (BE2C, $P < 0.0001$; 1643, $P < 0.0001$; EBC1, $P = 0.51$). B, the reduction in tumor proliferation observed in sensitive lines was confirmed by Ki67 staining of resected xenografts, and inhibition of CDK4/6 activity was confirmed by (C) immunohistochemical staining and Western blot for pRB^{S780}.

Discussion

Cure rates for children with high-risk neuroblastoma have not significantly improved over the last decade, and of those children who do achieve remission, half will ultimately suffer a relapse (1). Such unfavorable outcomes are due in part to the fact that the current treatment regimen does not sufficiently leverage the unique biological features of this heterogeneous disease. Indeed, although *MYCN* amplification is the most common genomic lesion in this disease, strategies to target this oncogene have not yet

resulted in a clinical deliverable. In addition, although the discovery that 8% to 10% of neuroblastomas harbor somatic activating mutations in the *ALK* oncogene provides another therapeutic opportunity (30, 31), most neuroblastoma patients will not have a somatic *ALK* mutation that is actionable with a targeted inhibitor (32–35). Steps must therefore be taken to identify additional molecular abnormalities that drive neuroblastoma disease progression and to subsequently exploit them with targeted therapy.

The data presented here identify CDK4/6 inhibition as a viable therapeutic strategy in neuroblastoma, with selectivity for patients whose tumors harbor *MYCN* amplification. Specifically, we show that RB phosphorylation via CDK4/6 signaling is nearly ubiquitous in neuroblastoma cell lines and tumors and is likely the result of high expression of *CDK4*, *CDK6*, and *CCND1* (ref. 15; Fig. 1), but there may be other as yet undiscovered mechanisms of CDK4/6 hyperactivation. However, despite the fact that CDK4/6 signaling is hyperactive in the majority of neuroblastoma cell lines, not all are sensitive to LEE011. Therefore, although the finding that a *CDK4*-amplified cell line (NGP) was highly sensitive to LEE011 may be clinically relevant, our data suggest that pRB, CDK4, or CDK6 status alone cannot be used to accurately predict a response to CDK4/6 inhibition. We instead show that sensitivity correlated significantly with *MYCN* amplification status. Indeed, cell lines displaying sensitivity to CDK4/6 inhibition by either siRNA-mediated depletion or LEE011 treatment were likely to be *MYCN* amplified (Figs. 2A and 3A) as well as harbor high MYCN mRNA and protein levels (Supplementary Fig. S3). Although MYC-induced replicative stress may be a contributing factor, the precise mechanism for this association is unknown. Nevertheless, the finding has important clinical ramifications, as CDK4/6 inhibition may provide an alternative therapy for the 40% of high-risk neuroblastoma cases harboring amplification at the *MYCN* locus. Future research, however, should focus on the discovery of additional biomarkers of sensitivity as a means to identify a sensitive patient population beyond *MYCN* or *CDK4* amplification status.

Over the last decade, first-generation CDK inhibitors have been evaluated in clinical trials for the treatment of adult malignancies, and a number of second-generation CDK inhibitors are currently undergoing phase I and phase II testing (7, 36). No clinical trial, however, has been adapted for childhood malignancies. As we show that CDK4/6 inhibition induces a cytostatic as opposed to a cytotoxic effect on neuroblastoma growth, combination strategies with conventional cytotoxic agents that rely on S-phase DNA replication may be antagonistic (37), suggesting that CDK4/6 inhibition may be best placed in the post-chemotherapy maintenance phase of treatment (immunotherapy and retinoids). Novel–novel screens with other agents that do not rely on targeted DNA replication should therefore be explored in order to develop a combinatorial strategy that will maximally inhibit the growth of residual, chemo-resistant cells. Taken together, our data suggest that a subset of neuroblastomas are highly sensitive to CDK4/6 inhibition, and support the clinical development of LEE011 in this disease.

Disclosure of Potential Conflicts of Interest

J.M. Maris has commercial research grant in Novartis. He is also a consultant/advisory board member of Novartis. No potential conflicts of interest were disclosed by the other authors.

Authors' Contributions

Conception and design: J. Rader, M. Russell, L.S. Hart, E.L. Carpenter, G. Caponigro, R.W. Schnepp, K.A. Cole, J.M. Maris
Development of methodology: J. Rader, M. Russell, M.S. Nakazawa, E.L. Carpenter, A.C. Wood, J.M. Maris
Acquisition of data (provided animals, acquired and managed patients, provided facilities, etc.): J. Rader, M.S. Nakazawa, L.T. Belcastro, D. Martinez, S. Parasuraman, G. Caponigro, B.R. Pawel, J.M. Maris
Analysis and interpretation of data (e.g., statistical analysis, biostatistics, computational analysis): J. Rader, L.S. Hart, Y. Li, E.L. Carpenter, E. F. Attiyeh, S.J. Diskin, S. Kim, S. Parasuraman, A.C. Wood, J.M. Maris
Writing, review, and/or revision of the manuscript: J. Rader, M. Russell, L.S. Hart, M.S. Nakazawa, E.F. Attiyeh, S. Parasuraman, G. Caponigro, R.W. Schnepp, A.C. Wood, K.A. Cole, J.M. Maris
Administrative, technical, or material support (i.e., reporting or organizing data, constructing databases): J. Rader, D. Martinez, J.M. Maris
Study supervision: L.S. Hart, K.A. Cole, J.M. Maris

Acknowledgments

The authors thank investigators in the neuroblastoma Therapeutically Applicable Research to Generate Effective Treatments (TARGET) consortium (ocg.cancer.gov/programs/target/projects/neuroblastoma) and especially Dr. S. Asgarzadeh and Dr. R. Seeger for generation of the patient gene expression data.

Grant Support

This work was generously supported through research grants from the Cookies for Kids Cancer, Arms Wide Open, Rally, and Alex's Lemonade Stand Foundations. R.W. Schnepp was supported by NIH Grant No. T32CA009615.

The costs of publication of this article were defrayed in part by the payment of page charges. This article must therefore be hereby marked *advertisement* in accordance with 18 U.S.C. Section 1734 solely to indicate this fact.

Received June 20, 2013; revised August 14, 2013; accepted August 29, 2013; published OnlineFirst September 17, 2013.

References

1. Cole KA, Maris JM. New strategies in refractory and recurrent neuroblastoma: translational opportunities to impact patient outcome. Clin Cancer Res 2012;18:2423–8.
2. Maris JM. Recent advances in neuroblastoma. N Engl J Med 2010; 362:2202–11.
3. Maris JM, Hogarty MD, Bagatell R, Cohn SL. Neuroblastoma. Lancet 2007;369:2106–20.
4. Carpenter EL, Mosse YP. Targeting ALK in neuroblastoma—preclinical and clinical advancements. Nat Rev Clin Oncol 2012;9:391–9.
5. Harbour JW, Luo RX, Dei Santi A, Postigo AA, Dean DC. Cdk phosphorylation triggers sequential intramolecular interactions that progressively block Rb functions as cells move through G1. Cell 1999; 98:859–69.
6. Malumbres M, Barbacid M. Cell cycle, CDKs and cancer: a changing paradigm. Nat Rev Cancer 2009;9:153–66.
7. Musgrove EA, Caldon CE, Barraclough J, Stone A, Sutherland RL. Cyclin D as a therapeutic target in cancer. Nat Rev Cancer 2011;11: 558–72.

8. Anders L, Ke N, Hydbring P, Choi YJ, Widlund HR, Chick JM, et al. A systematic screen for CDK4/6 substrates links FOXM1 phosphorylation to senescence suppression in cancer cells. Cancer Cell 2011;20:620–34.
9. Easton J, Wei T, Lahti JM, Kidd VJ. Disruption of the cyclin D/cyclin-dependent kinase/INK4/retinoblastoma protein regulatory pathway in human neuroblastoma. Cancer Res 1998;58:2624–32.
10. Krasnoselsky AL, Whiteford CC, Wei JS, Bilke S, Westermann F, Chen QR, et al. Altered expression of cell cycle genes distinguishes aggressive neuroblastoma. Oncogene 2005;24:1533–41.
11. Molenaar JJ, Koster J, Ebus ME, van Sluis P, Westerhout EM, de Preter K, et al. Copy number defects of G1-cell cycle genes in neuroblastoma are frequent and correlate with high expression of E2F target genes and a poor prognosis. Genes Chromosomes Cancer 2012;51:10–9.
12. Molenaar JJ, van Sluis P, Boon K, Versteeg R, Caron HN. Rearrangements and increased expression of cyclin D1 (CCND1) in neuroblastoma. Genes Chromosomes Cancer 2003;36:242–9.
13. Mosse YP, Diskin SJ, Wasserman N, Rinaldi K, Attiyeh EF, Cole K, et al. Neuroblastomas have distinct genomic DNA profiles that predict clinical phenotype and regional gene expression. Genes Chromosomes Cancer 2007;46:936–49.
14. Mosse YP, Greshock J, Margolin A, Naylor T, Cole K, Khazi D, et al. High-resolution detection and mapping of genomic DNA alterations in neuroblastoma. Genes Chromosomes Cancer 2005;43:390–403.
15. Molenaar JJ, Ebus ME, Koster J, van Sluis P, van Noesel CJ, Versteeg R, et al. Cyclin D1 and CDK4 activity contribute to the undifferentiated phenotype in neuroblastoma. Cancer Res 2008;68:2599–609.
16. Cole KA, Huggins J, Laquaglia M, Hulderman CE, Russell MR, Bosse K, et al. RNAi screen of the protein kinome identifies checkpoint kinase 1 (CHK1) as a therapeutic target in neuroblastoma. Proc Natl Acad Sci U S A 2011;108:3336–41.
17. Attiyeh EF, Diskin SJ, Attiyeh MA, Mosse YP, Hou C, Jackson EM, et al. Genomic copy number determination in cancer cells from single nucleotide polymorphism microarrays based on quantitative genotyping corrected for aneuploidy. Genome Res 2009;19:276–83.
18. Peddinti R, Zeine R, Luca D, Seshadri R, Chlenski A, Cole K, et al. Prominent microvascular proliferation in clinically aggressive neuroblastoma. Clin Cancer Res 2007;13:3499–506.
19. Russell M, Levin K, Rader J, Belcastro L, Li Y, Martinez D, et al. Combination therapy targeting the Chk1 and Wee1 kinases demonstrates therapeutic efficacy in neuroblastoma. Cancer Res 2013;73:776–84.
20. Bagatell R, London WB, Wagner LM, Voss SD, Stewart CF, Maris JM, et al. Phase II study of irinotecan and temozolomide in children with relapsed or refractory neuroblastoma: a Children's Oncology Group study. J Clin Oncol 2011;29:208–13.
21. Knudsen ES, Wang JY. Differential regulation of retinoblastoma protein function by specific Cdk phosphorylation sites. J Biol Chem 1996;271:8313–20.
22. Connell-Crowley L, Harper JW, Goodrich DW. Cyclin D1/Cdk4 regulates retinoblastoma protein-mediated cell cycle arrest by site-specific phosphorylation. Mol Biol Cell 1997;8:287–301.
23. Kitagawa M, Higashi H, Jung HK, Suzuki-Takahashi I, Ikeda M, Tamai K, et al. The consensus motif for phosphorylation by cyclin D1-Cdk4 is different from that for phosphorylation by cyclin A/E-Cdk2. EMBO J 1996;15:7060–9.
24. Burkhart DL, Sage J. Cellular mechanisms of tumour suppression by the retinoblastoma gene. Nat Rev Cancer 2008;8:671–82.
25. Chicas A, Wang X, Zhang C, McCurrach M, Zhao Z, Mert O, et al. Dissecting the unique role of the retinoblastoma tumor suppressor during cellular senescence. Cancer Cell 2010;17:376–87.
26. Harbour JW, Dean DC. Rb function in cell-cycle regulation and apoptosis. Nat Cell Biol 2000;2:E65–7.
27. Ruas M, Gregory F, Jones R, Poolman R, Starborg M, Rowe J, et al. CDK4 and CDK6 delay senescence by kinase-dependent and p16INK4a-independent mechanisms. Mol Cell Biol 2007;27:4273–82.
28. Wierstra I, Alves J. Transcription factor FOXM1c is repressed by RB and activated by cyclin D1/Cdk4. Biol Chem 2006;387:949–62.
29. Wang Z, Park HJ, Carr JR, Chen YJ, Zheng Y, Li J, et al. FoxM1 in tumorigenicity of the neuroblastoma cells and renewal of the neural progenitors. Cancer Res 2011;71:4292–302.
30. Bresler SC, Wood AC, Haglund EA, Courtright J, Belcastro LT, Plegaria JS, et al. Differential inhibitor sensitivity of anaplastic lymphoma kinase variants found in neuroblastoma. Sci Transl Med 2011;3:108ra14.
31. Mosse YP, Laudenslager M, Longo L, Cole KA, Wood A, Attiyeh EF, et al. Identification of ALK as a major familial neuroblastoma predisposition gene. Nature 2008;455:930–5.
32. Cheung NK, Zhang J, Lu C, Parker M, Bahrami A, Tickoo SK, et al. Association of age at diagnosis and genetic mutations in patients with neuroblastoma. JAMA 2012;307:1062–71.
33. Molenaar JJ, Koster J, Zwijnenburg DA, van Sluis P, Valentijn LJ, van der Ploeg I, et al. Sequencing of neuroblastoma identifies chromothripsis and defects in neuritogenesis genes. Nature 2012;483:589–93.
34. Pugh TJ, Morozova O, Attiyeh EF, Asgharzadeh S, Wei JS, Auclair D, et al. The genetic landscape of high-risk neuroblastoma. Nat Genet 2013;45:279–84.
35. Sausen M, Leary RJ, Jones S, Wu J, Reynolds CP, Liu X, et al. Integrated genomic analyses identify ARID1A and ARID1B alterations in the childhood cancer neuroblastoma. Nat Genet 2013;45:12–7.
36. Canavese M, Santo L, Raje N. Cyclin dependent kinases in cancer: potential for therapeutic intervention. Cancer Biol Ther 2012;13:451–7.
37. Dean JL, McClendon AK, Knudsen ES. Modification of the DNA damage response by therapeutic CDK4/6 inhibition. J Biol Chem 2012;287:29075–87.